SUPER-RESOLUTION

FOR IMAGERY ENHANCEMENT
USING VARIATIONAL QUANTUM EIGENSOLVER

Ystallonne Alves
Boxcat Inc.
ystallonne@boxc.at

7th IEEE Global Conference on Signal and Information Processing (GlobalSIP)

Super-Resolution for Imagery Enhancement Using Variational Quantum Eigensolver

Ystallonne Alves

Department of Informatics and Applied Mathematics
Federal University of Rio Grande do Norte
ystallonne@ufrn.edu.br

Ottawa, ON
November, 2019

Agenda

Introduction

Introduction

- Super-Resolution

Figure 1: Estimating a High-Resolution (HR) version of an image based on a Low-Resolution (LR) input is a complex task described as Single Image Super Resolution (SISR) [1].

Introduction

- Face recognition;
- Surveillance systems;
- Medical imaging;
- Remote sensing;
- Astronomical images;
- Forensics;
- Multimedia industry and video enhancement.

Introduction

- RAISR: Rapid and Accurate Image Super Resolution (ROMANO; ISIDORO; MILANFAR, 2017).
- VQE: Variational Quantum Eigensolver (PERUZZO et al., 2014).

Related Method

Related Method // Global Filter Learning

RAISR: Rapid and Accurate Image Super Resolution (ROMANO; ISIDORO; MILANFAR, 2017).

- Global Filter Learning

$$\min_{\mathbf{h}} \sum_{i=1}^{L} \|\mathbf{A}_i\mathbf{h} - \mathbf{b}_i\|_2^2 \tag{1}$$

$$\min_{\mathbf{h}} \|\mathbf{Q}\mathbf{h} - \mathbf{V}\|_2^2 \tag{2}$$

Related Method // Global Filter Learning

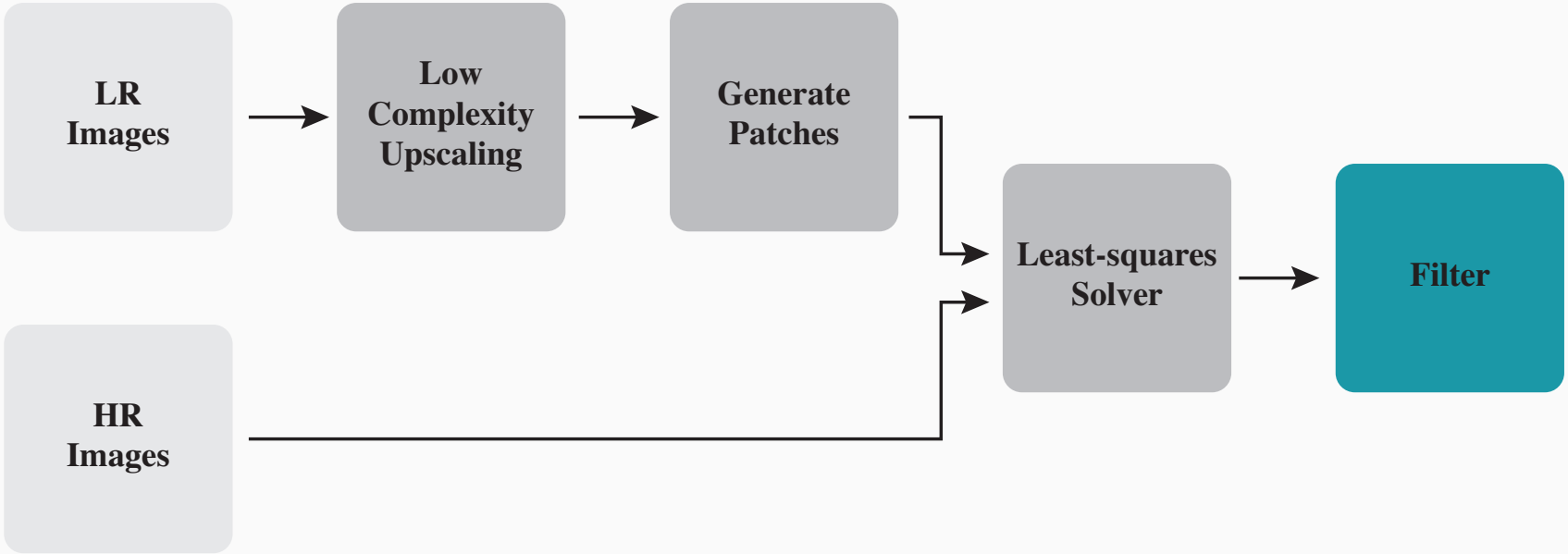

Figure 2: Learning stage.

Related Method // Global Filter Learning

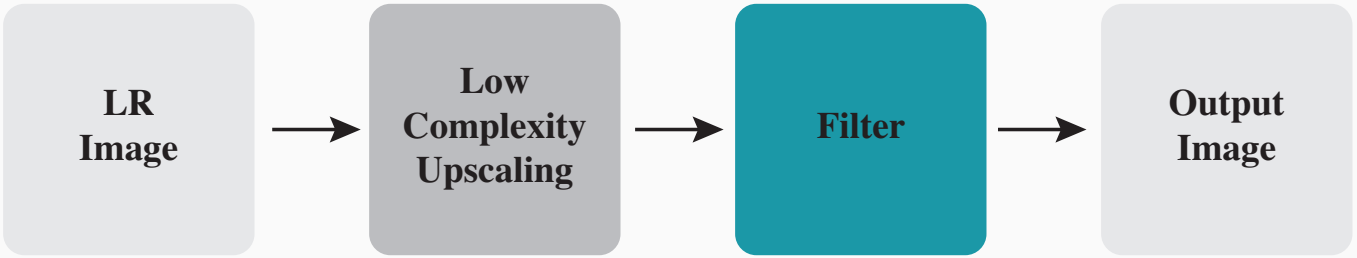

Figure 3: Upscaling stage.

Related Method // Global Filter Learning

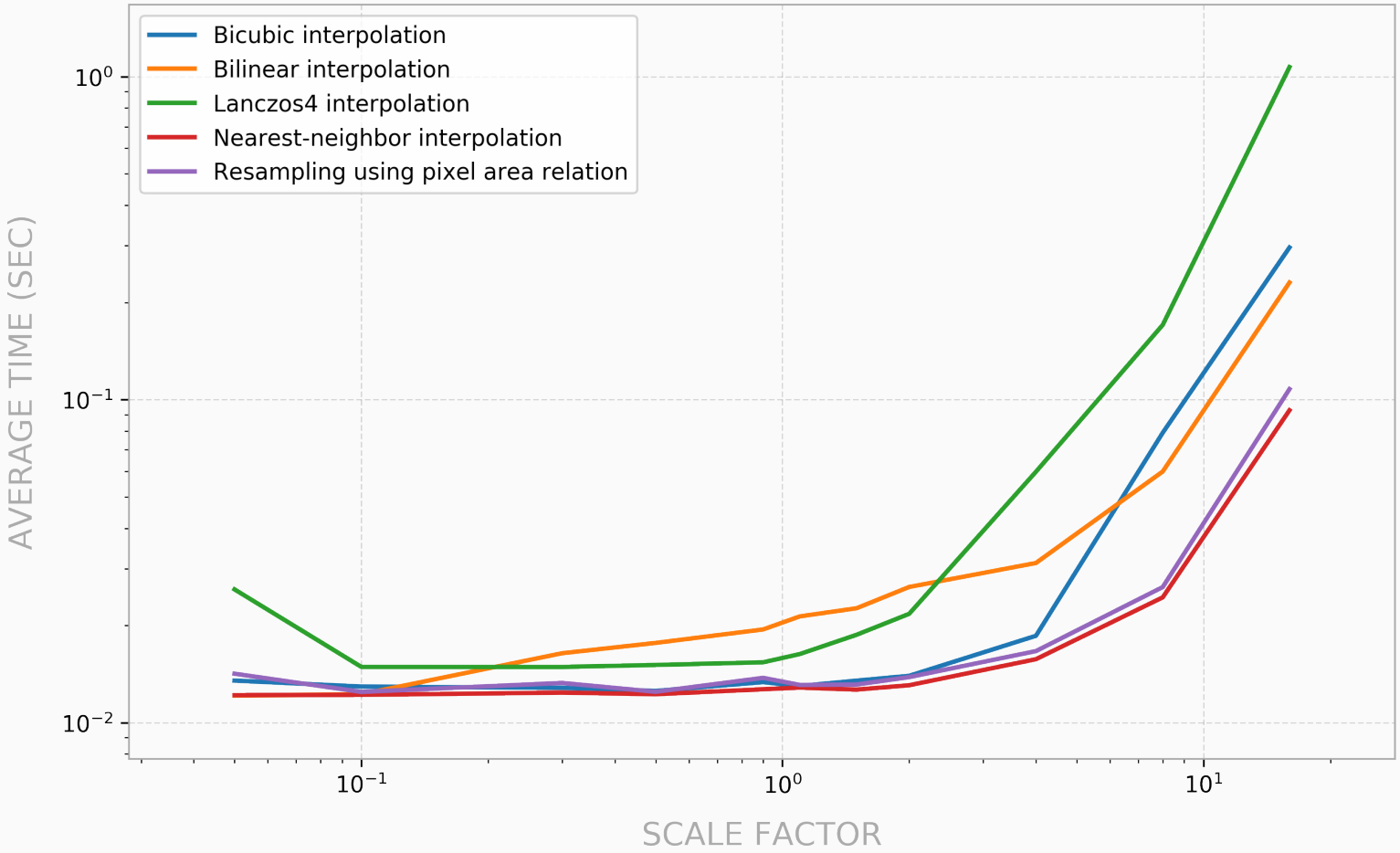

Figure 4: Speed performance comparison for traditional interpolation algorithms at several scale factors when resizing an input image from Set5 [51]. Nearest-neighbor consistently presents the best time performance for all scaling factors.

Related Method // Hashing-based Learning

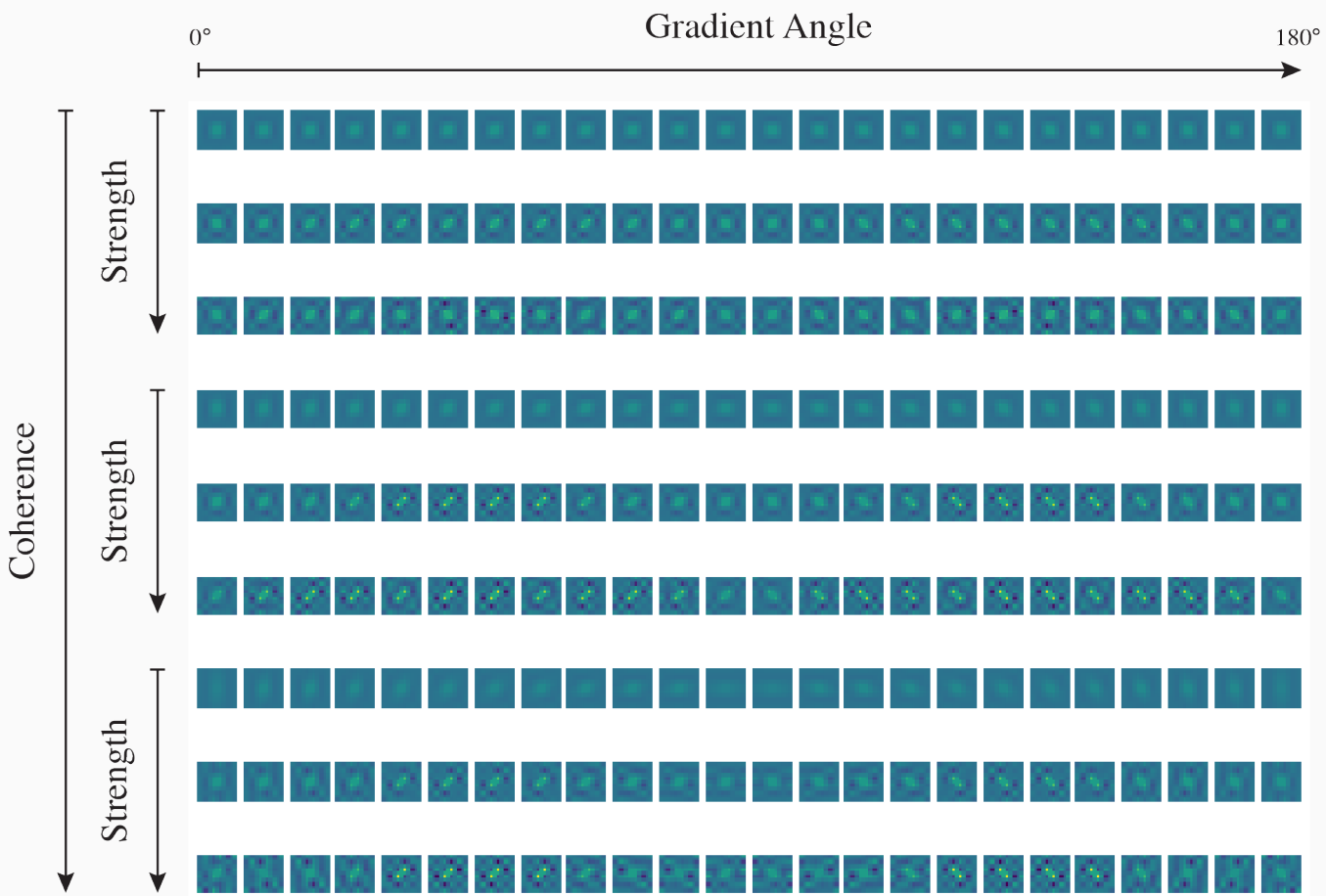

Figure 5: Visual representation for a single pixel type of a learned filter for a 2× upscaling factor.

Related Method // Local Gradient Statistics

- Local Gradient Statistics
  - Angle θ_k, Strength λ_1^k, and Coherence μ_k.

$$\mathbf{G}_k = \begin{bmatrix} g_{x_{k_1}} & g_{y_{k_1}} \\ \vdots & \vdots \\ g_{x_{k_n}} & g_{y_{k_n}} \end{bmatrix} \tag{3}$$

$$\mathbf{G}_k^T \mathbf{W}_k \mathbf{G}_k \tag{4}$$

$$\theta_k = \arctan(\phi_{1,y}^k, \phi_{1,x}^k), \quad \sqrt{\lambda_1^k}, \quad \mu_k = \frac{\sqrt{\lambda_1^k} - \sqrt{\lambda_2^k}}{\sqrt{\lambda_1^k} + \sqrt{\lambda_2^k}}. \tag{5}$$

Related Method // Classical Filter

- Classical Filter
  - Berkeley Segmentation Data Set and Benchmarks 500 (BSDS500) [50].

$$\mathbf{h}_{\alpha}$$

Proposed Method

Proposed Method // Variational Quantum Eigensolver

VQE: Variational Quantum Eigensolver (PERUZZO et al., 2014).

- Ground State Energy of the Hamiltonian **H**

$$\min_{\vec{\theta}} = \left\langle \psi(\vec{\theta}) \right| \mathbf{H} \left| \psi(\vec{\theta}) \right\rangle \tag{6}$$

Proposed Method // Variational Quantum Eigensolver

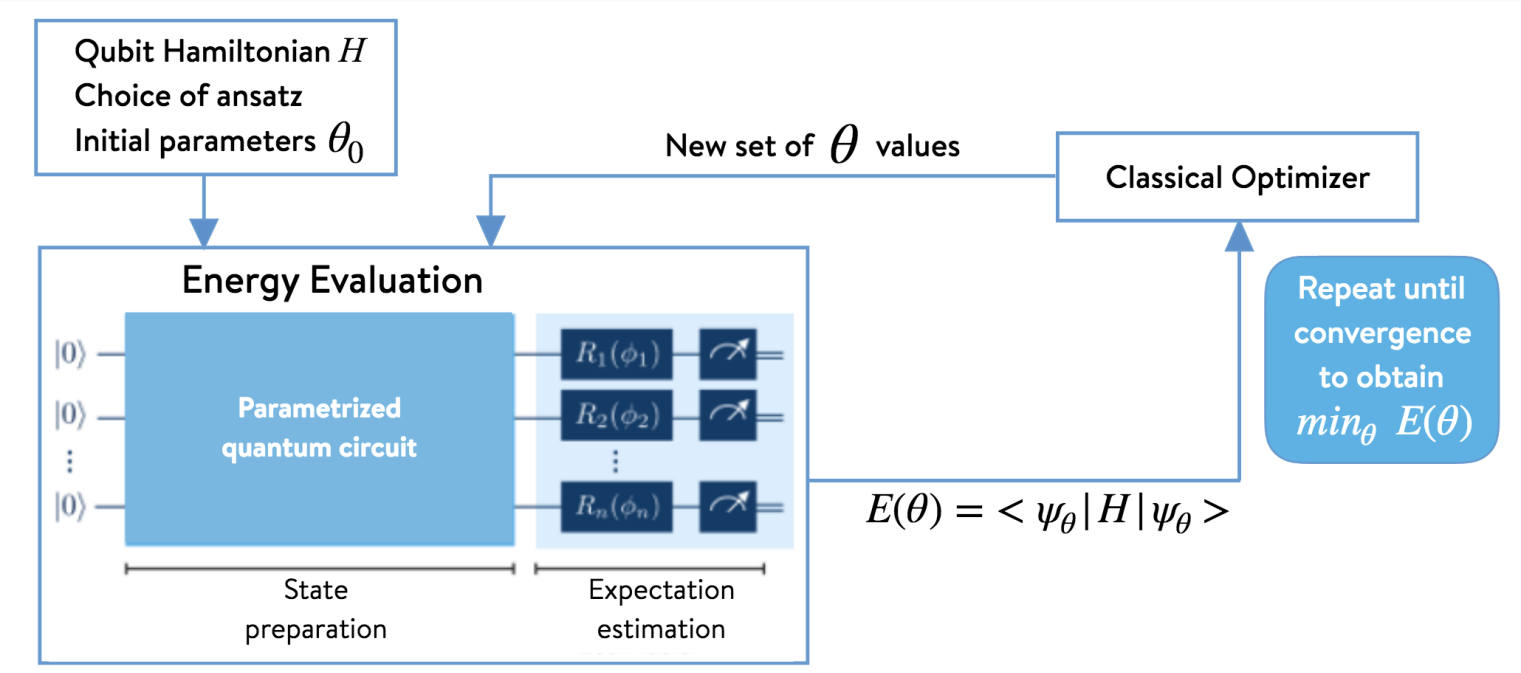

Figure 6: VQE Overview [19].

Proposed Method // Numerical Reference

- Numerical Reference

$$\mathbf{H} = \begin{cases} (0,0) & 1.345\,149\,691\,971\,852\,6 \times 10^{-4} \\ (0,1) & 2.421\,287\,807\,653\,396\,7 \times 10^{-5} \\ (1,0) & 2.421\,287\,807\,653\,396\,7 \times 10^{-5} \\ (1,1) & 2.436\,686\,682\,060\,184\,6 \times 10^{-4} \end{cases} \tag{7}$$

Proposed Method // Numerical Reference

- Exact Eigensolver (**EE**):

$$\mathbf{EE}\lambda_1^k = 0.000248798568458 9, \mathbf{EE}\phi_1^k = \begin{bmatrix} -0.207265847895268 4 \\ -0.978284656067064 8 \end{bmatrix}. \quad (8)$$

$$\mathbf{EE}\lambda_2^k = 0.000129385068944 3, \mathbf{EE}\phi_2^k = \begin{bmatrix} -0.978284656067064 8 \\ 0.207265847895268 4 \end{bmatrix}. \quad (9)$$

Proposed Method // Numerical Reference

$$\min_{\vec{\theta}} = |\mathbf{H}\rangle_{|\psi(\vec{\theta})\rangle} \geq \lambda_{min} \tag{10}$$

$$-\min_{\mathbf{x}} -f(x) = \max_{\mathbf{x}} f(x) \tag{11}$$

Proposed Method // Classical Optimization

- Classical Optimization:
  - ADAM;
  - Analytic Quantum Gradient Descent (AQGD);
  - Conjugate Gradient (CG) Method;
  - Constrained Optimization BY Linear Approximation (COBYLA);
  - Limited-memory Broyden-Fletcher-Goldfarb-Shanno Bound (L-BFGS-B);
  - Nelder-Mead (NM);
  - Sequential Least SQuares Programming (SLSQP);
  - Simultaneous Perturbation Stochastic Approximation (SPSA);
  - Truncated Newton (TNC).

Proposed Method // Classical Optimization

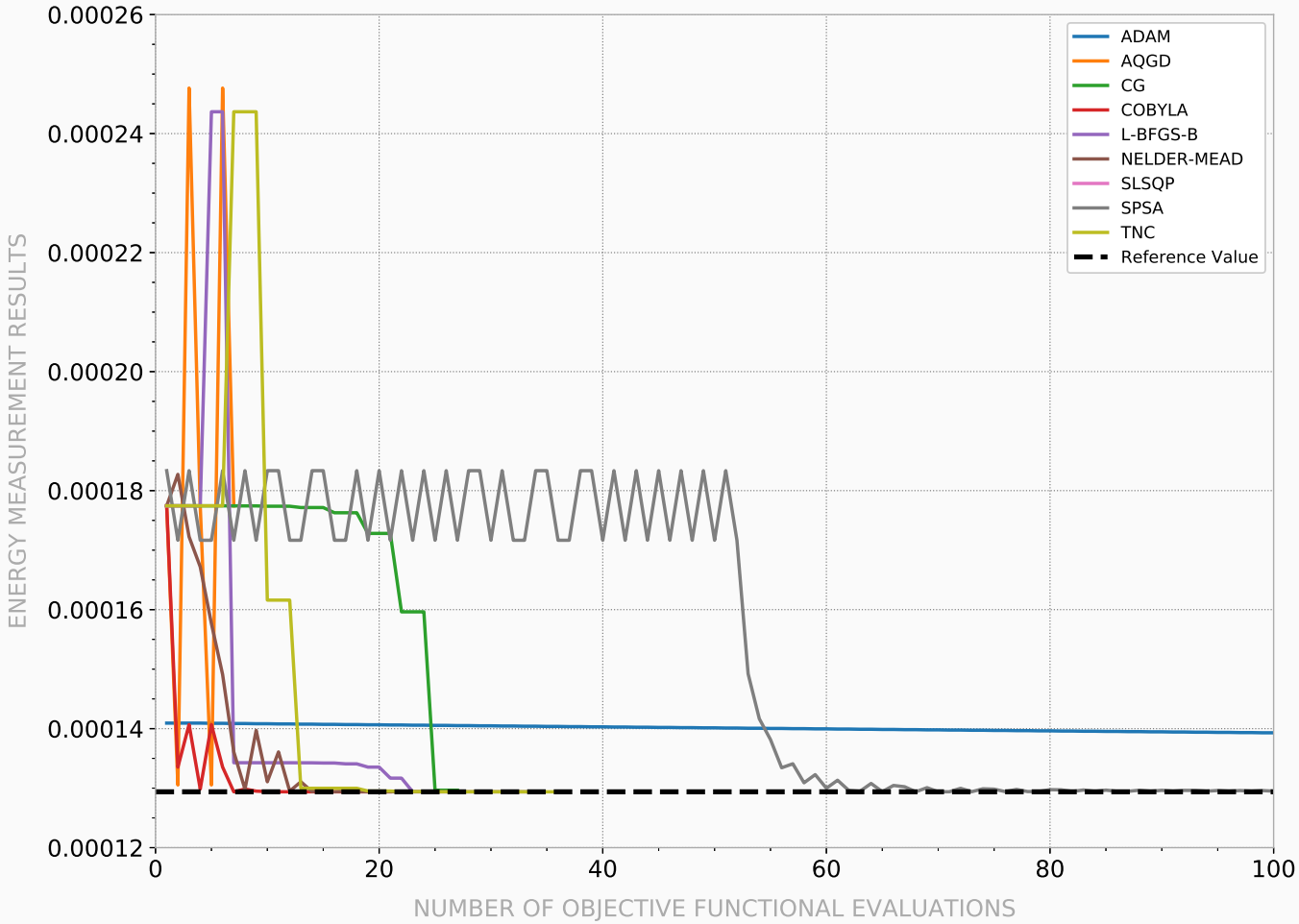

Figure 7: Energy convergence for local optimizers towards $\mathbf{EE}\lambda_k^2$.

Proposed Method // Classical Optimization

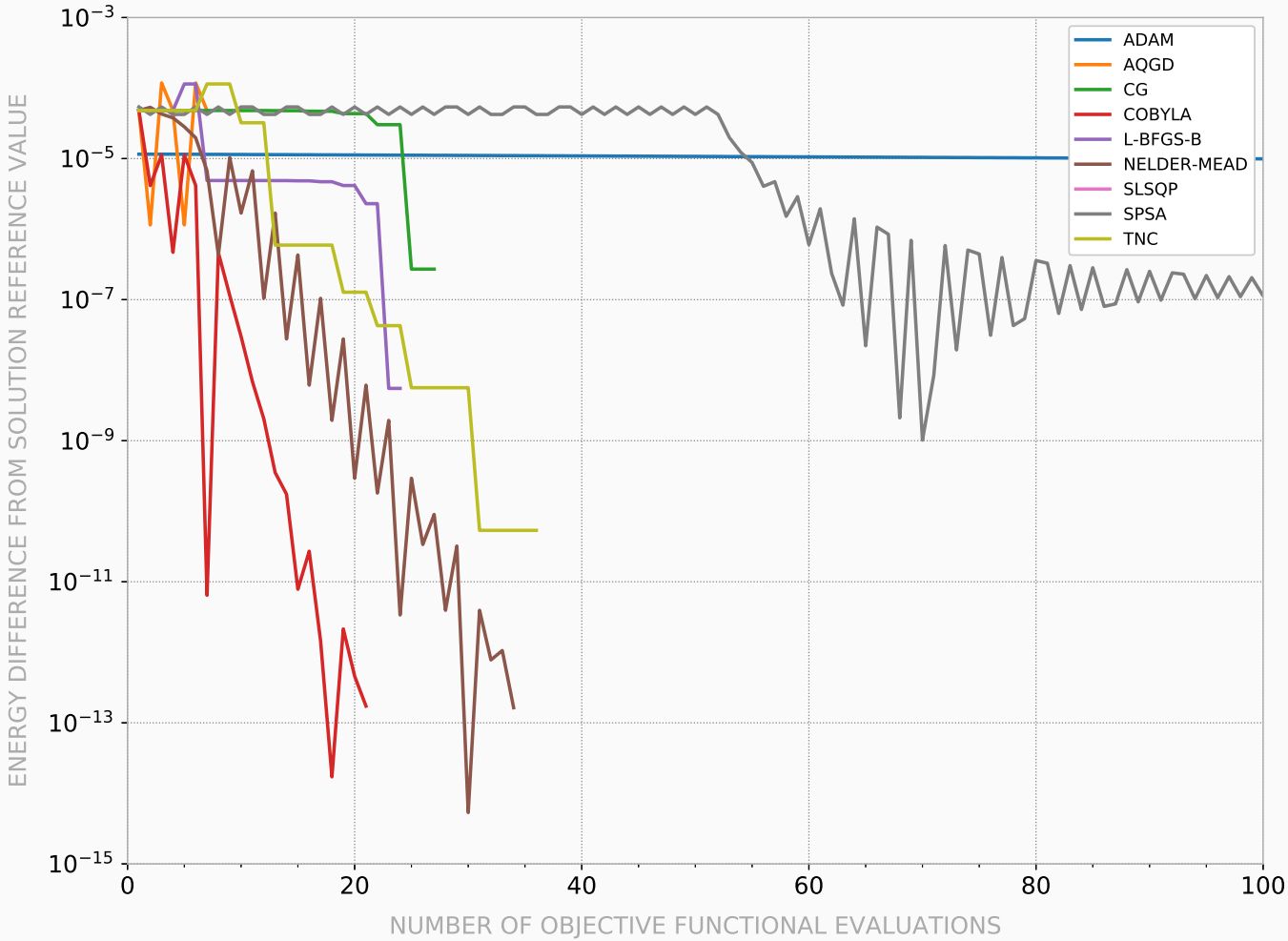

Figure 8: Divergence from reference value $\mathbf{EE}\lambda_k^2$.

Proposed Method // Classical Optimization

- COBYLA:

$$COBYLA\lambda_{max} = -0.00024879856832430445, \tag{12}$$

$$COBYLA\phi_{max} = \begin{bmatrix} -0.2072330078108220 \\ -0.9782916132082906 \end{bmatrix}. \tag{13}$$

- Exact Eigensolver:

$$EE\lambda_1^k = 0.0002487985684589, \tag{14}$$

$$EE\phi_1^k = \begin{bmatrix} -0.2072658478952684 \\ -0.9782846560670648 \end{bmatrix}. \tag{15}$$

Proposed Method // Classical Optimization

- COBYLA:

$$COBYLA\lambda_{min} = 0.00012938506911698078, \tag{16}$$

$$COBYLA\phi_{min} = \begin{bmatrix} 0.9782925363087142 \\ -0.2072286500526972 \end{bmatrix}. \tag{17}$$

- Exact Eigensolver:

$$EE\lambda_2^k = 0.0001293850689443, \tag{18}$$

$$EE\phi_2^k = \begin{bmatrix} -0.9782846560670648 \\ 0.2072658478952684 \end{bmatrix}. \tag{19}$$

Proposed Method // Classical Optimization

- Evolution Time (ET) in seconds for convergence to ground state considering 21 evaluations with COBYLA:

$$COBYLA\lambda_{max}ET = 4.131\,388\,664\,245\,605\,5 \times 10^{-2}, \tag{20}$$

$$COBYLA\lambda_{min}ET = 4.220\,700\,263\,977\,051 \times 10^{-2}. \tag{21}$$

Proposed Method // Classical Optimization

It took approximately 1 hour for all evaluations to be completed using a real device, with 3504 seconds for total Evaluation Time, considering 18 evaluations with COBYLA.

$$COBYLA\lambda_{min}^{\dagger} = 0.0001344612881702 4897. \tag{22}$$

Numerical References:

$$COBYLA\lambda_{min} = 0.0001293850691169 8078. \tag{23}$$

$$EE\lambda_{2}^{k} = 0.000129385068944 3. \tag{24}$$

Proposed Method // Quantum-Classical Filter

- Quantum-Classical Filter
  - Berkeley Segmentation Data Set and Benchmarks 500 (BSDS500) [50].

$$\mathbf{h}_{\beta}$$

Experimental Results

Experimental Results

Table 1: Quantitative comparison of the enhancement with several objective methods for the average performance result measured on the test images of Set5 [51].

Filter ($2\times$)	**MSE**	**PSNR**	**SSIM**	**VIF**	**RECO**
Reference Values	0.00	100.00	1.00	1.00	1.00
$\mathbf{h}_{\alpha}$ (Classical)	102.85	33.55	0.904	0.91	1.07
$\mathbf{h}_{\beta}$ (Quantum-Classical)	102.85	33.55	0.904	0.91	1.07

Remarks and Conclusion

Remarks and Conclusion

As with any nascent technology, there are limitations to the quantum computers and the simulators [24]. Time requirement to solve the complete operation using VQE could be decreased employing a generalization that reduces the number of samples [25] and the inherent parallelizability of the hybrid approach [26].

The classical optimization and the quantum computation are both parallelizable, with potential to overcome the more protracted runtime verified when comparing to the state-of-the-art, linearly improving per additional qubit.

Remarks and Conclusion

The concept of the VQE algorithm was first introduced in [2] with an implementation using integrated quantum photonics technology [27]. The VQE has the notable property that it can run on any quantum device [28], and it has already been experimentally demonstrated in other quantum platforms, including trapped ions [29] and superconducting circuits [30, 31].

This work benefits from the resources in the IBM Q Experience and the Quantum Information Science Kit – Qiskit [24], which conveniently includes the VQE algorithm.

Implementations of the VQE are also currently available in additional quantum computing and software platforms, such as in the ones offered by Rigetti Computing and Xanadu.

Acknowledgment

Acknowledgment

The author acknowledges IBM for granting quantum computing resources and cloud infrastructure that allowed further achievements with experiments in this work. He would also like to thank Bruno de Carvalho for timely assistance in guidance with insightful input. Equally, it is highly appreciated the support received from Creative Destruction Lab, Bloomberg Beta, DCVC, and Spectrum 28.

References

References i

[1] Y. Romano, J. Isidoro, and P. Milanfar, “RAISR: Rapid and Accurate Image Super Resolution,” IEEE Transactions on Computational Imaging, vol. 3, no. 1, pp. 110–125, Mar. 2017.

[2] A. Peruzzo et al., “A variational eigenvalue solver on a quantum processor,” Nat Commun, vol. 5, no. 1, p. 4213, Sep. 2014.

[3] S. Anwar, S. Khan, and N. Barnes, “A deep journey into super-resolution: a survey,” arXiv:1904.07523 [cs], Apr. 2019.

[4] S. Borman and R. L. Stevenson, “Super-resolution from image sequences - a review,” in 1998 Midwest Symposium on Circuits and Systems (Cat. No. 98CB36268), 1998, pp. 374–378.

[5] S. Farsiu, M. D. Robinson, M. Elad, and P. Milanfar, “Fast and robust multiframe super resolution,” IEEE Transactions on Image Processing, vol. 13, no. 10, pp. 1327–1344, Oct. 2004.

[6] R. Girshick, J. Donahue, T. Darrell, and J. Malik, “Region-based convolutional networks for accurate object detection and segmentation,” IEEE Transactions on Pattern Analysis and Machine Intelligence, vol. 38, no. 1, pp. 142–158, Jan. 2016.

[7] Y. Bai, Y. Zhang, M. Ding, and B. Ghanem, “SOD-MTGAN: Small Object Detection via Multi-Task Generative Adversarial Network,” in Computer Vision – ECCV 2018, 2018, pp. 210–226.

[8] S. P. Mudunuri and S. Biswas, “Low resolution face recognition across variations in pose and illumination,” IEEE Transactions on Pattern Analysis and Machine Intelligence, vol. 38, no. 5, pp. 1034–1040, May 2016.

References ii

[9] H. Greenspan, “Super-resolution in medical imaging,” Computer Journal, vol. 52, no. 1, pp. 43–63, Jan. 2009.

[10] T. Lillesand, R. W. Kiefer, and J. Chipman, Remote sensing and image interpretation, 7th ed. USA: John Wiley & Sons, Inc., 2015.

[11] A. P. Lobanov, “Resolution limits in astronomical images,” arXiv:astro-ph/0503225, Mar. 2005.

[12] A. Swaminathan, M. Wu, and K. J. R. Liu, “Digital image forensics via intrinsic fingerprints,” IEEE Transactions on Information Forensics and Security, vol. 3, no. 1, pp. 101–117, Mar. 2008.

[13] S. He and B. Jalali, “Brain MRI image super resolution using phase stretch transform and transfer learning,” arXiv:1807.11643 [cs], Jul. 2018.

[14] Y. Nakahara, T. Yamaguchi, and M. Ikehara, “Single image super-resolution with limited numbers of filters,” in 2018 IEEE Global Conference on Signal and Information Processing (GlobalSIP), Anaheim, CA, USA, 2018, pp. 36–40.

[15] X. Feng, P. Milanfar, “Multiscale principal components analysis for image local orientation estimation,” Proc. 36th AsilomarConf. Signals Syst. Comput., pp. 478–482, Nov. 2002.

[16] J. Preskill, “Quantum computing in the NISQ era and beyond,” Quantum, vol. 2, p. 79, Aug. 2018.

[17] J. Romero, R. Babbush, J. R. McClean, C. Hempel, P. Love, and A. Aspuru-Guzik, “Strategies for quantum computing molecular energies using the unitary coupled cluster ansatz,” arXiv:1701.02691 [quant-ph], Jan. 2017.

References iii

[18] G. Nannicini, “Performance of hybrid quantum/classical variational heuristics for combinatorial optimization,” Phys. Rev. E, vol. 99, no. 1, p. 013304, Jan. 2019.

[19] R. Q. Computing, “Grove documentation,” p. 71, Aug. 2018.

[20] R. Miceli and M. McGuigan, “Quantum computation and visualization of hamiltonians using discrete quantum mechanics and IBM Qiskit,” 2018 New York Scientific Data Summit (NYSDS), pp. 1–6, Aug. 2018.

[21] P. J. Coles et al., “Quantumn algorithm implementations for beginners,” arXiv:1804.03719 [quant-ph], Apr. 2018.

[22] “Qiskit Aqua: experimenting with max-cut problem and traveling salesman problem with variational quantum eigensolver.” [Online]. Available: http://bit.ly/MAXCUT-TSP. [Accessed: 24-Jun-2019].

[23] N. Moll et al., “Quantum optimization using variational algorithms on near-term quantum devices,” Quantum Sci. Technol., vol. 3, no. 3, p. 030503, Jul. 2018.

[24] G. Aleksandrowicz et al., “Qiskit: an open-source framework for quantum computing”. 2019.

[25] D. Wang, O. Higgott, and S. Brierley, “Accelerated variational quantum eigensolver,” Phys. Rev. Lett., vol. 122, no. 14, p. 140504, Apr. 2019.

[26] S. McArdle, S. Endo, A. Aspuru-Guzik, S. Benjamin, and X. Yuan, “Quantum computational chemistry,” arXiv:1808.10402 [quant-ph], Aug. 2018.

[27] J. L. O’Brien, A. Furusawa, and J. Vučković, “Photonic quantum technologies,” Nature Photon, vol. 3, no. 12, pp. 687–695, Dec. 2009.

References iv

[28] J. R. McClean, J. Romero, R. Babbush, and A. Aspuru-Guzik, “The theory of variational hybrid quantum-classical algorithms,” New J. Phys., vol. 18, no. 2, p. 023023, Feb. 2016.

[29] Y. Shen, X. Zhang, S. Zhang, J.-N. Zhang, M.-H. Yung, and K. Kim, “Quantum implementation of unitary coupled cluster for simulating molecular electronic structure,” Phys. Rev. A, vol. 95, no. 2, p. 020501, Feb. 2017.

[30] P. J. J. O’Malley et al., “Scalable quantum simulation of molecular energies,” Phys. Rev. X, vol. 6, no. 3, p. 031007, Jul. 2016.

[31] A. Kandala et al., “Hardware-efficient variational quantum eigensolver for small molecules and quantum magnets,” Nature, vol. 549, no. 7671, pp. 242–246, Sep. 2017.

[32] D. P. Kingma and J. Ba, “Adam: a method for stochastic optimization,” Dec. 2014.

[33] K. Mitarai, M. Negoro, M. Kitagawa, and K. Fujii, “Quantum circuit learning,” Phys. Rev. A, vol. 98, no. 3, p. 032309, Sep. 2018.

[34] J. Nocedal and S. Wright, Numerical optimization, 2nd ed. New York: Springer-Verlag, 2006.

[35] M. J. D. Powell, “A direct search optimization method that models the objective and constraint functions by linear interpolation,” in Advances in Optimization and Numerical Analysis, S. Gomez and J.-P. Hennart, Eds. Dordrecht: Springer Netherlands, 1994, pp. 51–67.

[36] M. J. D. Powell, “Direct search algorithms for optimization calculations,” Acta Numerica, vol. 7, pp. 287–336, Jan. 1998.

[37] R. H. Byrd, P. Lu, J. Nocedal, and C. Zhu, “A limited memory algorithm for bound constrained optimization,” SIAM J. Sci. Comput., vol. 16, no. 5, pp. 1190–1208, Sep. 1995.

References v

[38] C. Zhu, R. H. Byrd, P. Lu, and J. Nocedal, “Algorithm 778: L-BFGS-B: fortran subroutines for large-scale bound-constrained optimization,” ACM Trans. Math. Softw., vol. 23, no. 4, pp. 550–560, Dec. 1997.

[39] J. L. Morales and J. Nocedal, “Remark on ‘Algorithm 778: L-BFGS-B: fortran subroutines for large-scale bound constrained optimization,” ACM Trans. Math. Softw., vol. 38, no. 1, pp. 7:1–7:4, Dec. 2011.

[40] J. A. Nelder and R. Mead, “A simplex method for function minimization,” Comput J, vol. 7, no. 4, pp. 308–313, Jan. 1965.

[41] D. Kraft, “A software package for sequential quadratic programming,” Institute for Flight Mechanics, DLR German Aerospace Center, Koln, Germany, Technical Report DFVLR-FB 88–28, Jul. 1988.

[42] J. C. Spall, “Multivariate stochastic approximation using a simultaneous perturbation gradient approximation,” IEEE Transactions on Automatic Control, vol. 37, no. 3, pp. 332–341, Mar. 1992.

[43] S. Nash, “Preconditioning of truncated-Newton methods,” SIAM J. Sci. and Stat. Comput., vol. 6, no. 3, pp. 599–616, Jul. 1985.

[44] S. Nash, “Newton-type minimization via the Lanczos Method,” SIAM J. Numer. Anal., vol. 21, no. 4, pp. 770–788, Aug. 1984.

[45] I. Begin and F. P. Ferrie, “Comparison of super-resolution algorithms using image quality measures,” in 3rd Canadian Conference on Computer and Robot Vision, 2006, p. 72.

References vi

[46] H. R. Sheikh and A. C. Bovik, “Image information and visual quality,” IEEE Transactions on Image Processing, vol. 15, no. 2, pp. 430–444, 2006.

[47] Z. Wang and Q. Li, “Information content weighting for perceptual image quality assessment,” IEEE Transactions on Image Processing, vol. 20, no. 5, pp. 1185–1198, May 2005.

[48] K. Nasrollahi and T. B. Moeslund, “Super-resolution: a comprehensive survey,” Machine Vision and Applications, May 2014.

[49] V. Baroncini, L. Capodiferro, E. D. D. Claudio, and G. Jacovitti, “The polar edge coherence: a quasi blind metric for video quality assessment,” EUSIPCO, pp. 564–568, 2009.

[50] P. Arbelaez, M. Maire, C. Fowlkes, and J. Malik, “Contour detection and hierarchical image segmentation,” IEEE Transactions on Pattern Analysis and Machine Intelligence, vol. 33, no. 5, pp. 898–916, May 2011.

[51] M. Bevilacqua, A. Roumy, C. Guillemot, and M. A. Morel, “Low-complexity single-image super-resolution based on nonnegative neighbor embedding,” in Proceedings of the British Machine Vision Conference, 2012, pp. 135.1–135.10.